Characterization of a Novel 100-Channel Silicon Photomultiplier—Part II: Charge and Time

Paolo Finocchiaro, Alfio Pappalardo, Luigi Cosentino, Massimiliano Belluso, Sergio Billotta, Giovanni Bonanno, Beatrice Carbone, Giovanni Condorelli, Salvatore Di Mauro, Giorgio Fallica, Massimo Mazzillo, Alessandro Piazza, Delfo Sanfilippo, and Giuseppina Valvo

***Abstract*—In this paper, we present the results of the charge and time characterization performed on our novel 100-channel silicon photomultiplier. We have improved our previous single-photon-avalanche-diode technology in order to set up a working device with outstanding features in terms of single-photon resolving power up to $R = 45$, a timing resolution down to 100 ps, and photon-detection efficiency of 14% at 420 nm. Tests were performed, and features were measured as a function of the bias voltage and of the incident photon flux. A dedicated data analysis procedure was developed that allows to extract at once the relevant parameters from the amplitude spectra and to determine the timing features.**

***Index Terms*—Afterpulsing, dark noise, gain, quantum detection efficiency, quenching resistor, silicon photomultiplier (SiPM), single-photon avalanche photodiode, single-photon counting.**

I. Introduction

PHOTON handling is nowadays considered an emerging issue, with many possible applications, particularly in the wide field of sensors and related transducers [1]. Throughout the last years, a new kind of planar semiconductor device has slowly but steadily come out, namely, the silicon photomultiplier (SiPM), with promising features that, in some respect, could even replace traditional photomultiplier tubes [2]. Based on a Geiger-mode avalanche photodiode elementary cell [3], it consists of an array of n independent identical microcells whose outputs are connected together. The final output is thus the analog superposition of n ideally binary signals [4]–[6]. This scheme, along with the sensitivity of each individual cell to single photons, appears to result (in principle) in the perfect photosensor capable of detecting and counting the single photons in a light pulse.

Unfortunately, this is not the case, as this kind of device has several drawbacks, all of them mainly deriving from its noise features, as already shown in part 1 of this paper. Nonetheless, the suitable use of SiPMs depends strongly on the particular application; although dark counts are a problem for low-level light applications, if there is ample light, one can set the threshold at several photoelectrons and, thus, suppress them. Such a tradeoff can be useful to optimize the energy resolution.

Therefore, although not capable of totally replacing the traditional photomultiplier tubes, the SiPM already promises to fulfill a wide set of requirements coming from numerous applications. This is why many groups and companies are currently working toward large-area SiPMs [7]–[16].

In previous papers, we described our development and test of single channels and arrays of 5×5 single-photon avalanche diodes (SPADs) operating at low voltage and fabricated in silicon planar technology [17]–[20]. In this paper, we will illustrate the characterization of our novel 10×10 SiPM, which is already described in part 1, in terms of charge, time resolution, and photon-detection efficiency (PDE). We will show that the device performance is indeed outstanding, although it still represents the first-generation prototype and other better performing sensors are already under production.

II. Low-Light-Level Characterization

In order to characterize the device response with respect to a low level of incident light and to the bias voltage, we employed the setup shown in Fig. 1. We put our SiPM into a light-tight box and positioned the fiber coming from the laser just in front of it, making sure that the laser spot was covering the whole active area. This optomechanical setup was fixed for the whole duration of the tests, ensuring that although absolute measurements were not possible, all the measurements can be compared with and scaled to each other.

After carefully verifying the repeatability of the results, we started our test by running the system at the four predefined bias values with nominal laser intensities of 6%, 7%, 8%, 9%, and 10%. Unfortunately, the measurements at 10% were only possible for two bias values, due to a technical problem. The laser repetition rate was fixed at 1 kHz.

A. Charge Response

As mentioned in Section I, the ideal charge output of the SiPM should approximate digital information, i.e., a signal which is an integer multiple of the elementary cell output,

Manuscript received July 16, 2008. Current version published September 24, 2008. The review of this paper was arranged by Editor C. Nguyen.

P. Finocchiaro and L. Cosentino are with the Laboratori Nazionali del Sud, INFN, 95125 Catania, Italy (e-mail: finocchiaro@infn.lns.infn.it).

A. Pappalardo is with the Laboratori Nazionali del Sud, INFN, 95125 Catania, Italy, and also with STMicroelectronics, 95121 Catania, Italy.

M. Belluso, G. Bonanno, and S. Di Mauro are with the Osservatorio Astronomico di Catania, INAF, 95125 Catania, Italy.

S. Billotta is with the Osservatorio Astronomico di Catania, INAF, 95125 Catania, Italy, and also with STMicroelectronics, 95121 Catania, Italy.

B. Carbone, G. Condorelli, G. Fallica, M. Mazzillo, A. Piazza, D. Sanfilippo, and G. Valvo are with the R&D DSG, STMicroelectronics, 95121 Catania, Italy.

Color versions of one or more of the figures in this paper are available online at http://ieeexplore.ieee.org.

Digital Object Identifier 10.1109/TED.2008.2003235

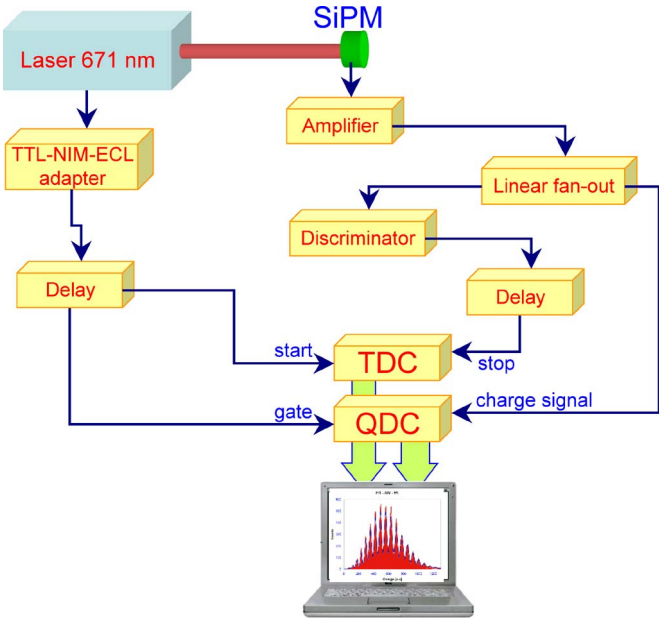

Fig. 1. Sketch of the electronics for the charge and time measurements employed for SiPM response characterization.

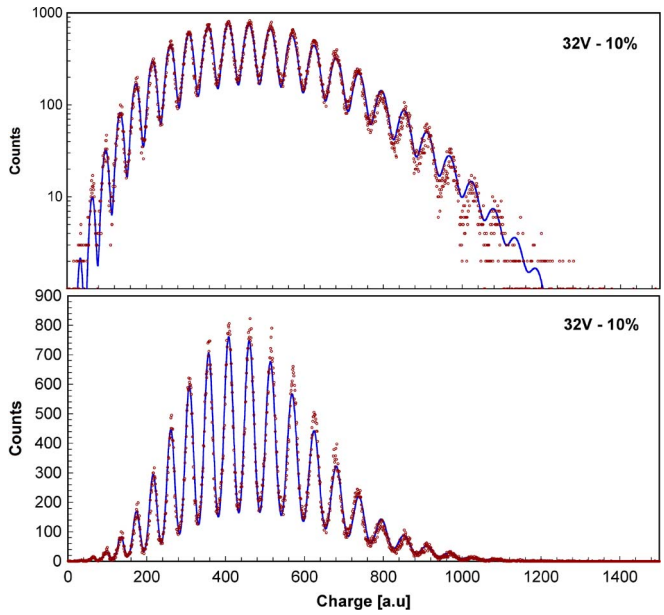

Fig. 2. Sample charge spectrum from the SiPM biased at 32 V and under a nominal laser intensity of 10%, shown in (upper plot) logarithmic and (lower plot) linear scales. The circles are data points; the line is the result of a fit, as explained in the text.

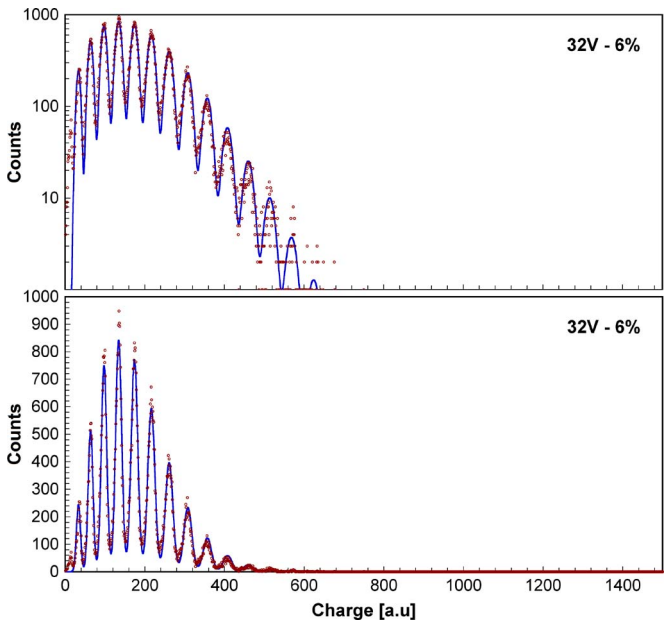

Fig. 3. Sample charge spectrum from the SiPM biased at 32 V and under a nominal laser intensity of 6%, shown in (upper plot) logarithmic and (lower plot) linear scales. The circles are data points; the line is the result of a fit, as explained in the text.

depending on the number of detected photons. This, of course, only holds in the ideal case because of several reasons.

1) Small differences between individual cells may result in variations of the output signal.
2) Electrical noise, uncorrelated dark counts, afterpulses, and crosstalk can perturb the output-signal shape.
3) A photon interacting with a cell while it is recharging gives rise to a smaller signal.
4) A photon interacting in a boundary region between cells or at the wrong depth may give rise to a smaller and/or delayed signal.

For all of the aforementioned reasons, what one expects as an SiPM charge spectrum when it is illuminated with a low-intensity time-coherent laser pulse is an overall Poisson distribution possibly modulated with peaks related to integer numbers of detected photons. This is just what we found, as shown in the examples of Figs. 2 and 3 for two different light levels (10% and 6% nominal laser intensity). We note that at low light level, an additional peak appears below the one attributed to one detected photon. Such a peak, usually called pedestal and whose position is not evenly spaced with respect to the other peaks, is due to the nonnegligible probability of detecting zero photons. In such a case, although the laser trigger starts the data acquisition, the charge to digital converter only integrates the baseline level, giving rise to a pedestal count.

In Figs. 2 and 3, the data points are represented by circles, whereas the continuous line represents the result of a fit procedure that we are going to describe. As mentioned earlier, the expected dominant contribution to the distribution of the charge signal from the SiPM, when illuminated with low-intensity laser pulses, is a Poisson one. Obviously, the Poisson distribution is a discrete one; however, due to the mentioned effects, each single value is smeared in a Gaussian fashion. The width of each peak (see Figs. 2 and 3) is expected to basically depend on two factors:

a) the overall electronic noise of the detector and of the electronics, which we suppose to be constant over the set of measurements;
b) the combination of nonuniformities and fluctuations between all the elementary cells, resulting in a contribution that should scale with the square root of the number of responding cells.

Therefore, the overall variance of the nth peak is expected to be

$$\sigma^2_{\rm tot}(n) = \sigma^2_e + n\sigma^2_1 \tag{1}$$

where σ_e represents the contribution a) and σ_1 is the Gaussian width of the contribution b) to the first peak.

The spectrum shape is then expected to be the convolution of a Poisson distribution with several peaks, whose width is given by (1), which can be expressed as follows:

$$F(x) = A\frac{dP}{dx} = A\cdot\sum_{n=1}^{\infty}{\rm Poisson}(\mu,n) \cdot\frac{1}{\sigma_{\rm tot}(n)\sqrt{2\pi}}\cdot e^{-\frac{[x-c(n)]^2}{2\sigma^2_{\rm tot}(n)}}. \tag{2}$$

A is a normalization constant, which is equal to the integral of the measured spectrum.

μ is the average value of the Poisson distribution.

$c(n)$ is a stepwise function expressing the coordinate of the centroid of the n peaks. In principle, one would expect that the $c(n)$ values lie on a straight line; however, this is only roughly the case. Indeed, the QDC response is affected by the differential nonlinearity (DNL), i.e., the real width of each bin fluctuates while going from the start to the end of the conversion scale. Therefore, although the overall behavior of the QDC is claimed to be linear within $\pm 0.05\%$ of a full scale, the local nonlinearity is only below $\pm 1\%$ based on the specifications of the manufacturer. This means that the expected equally spaced peaks' pattern could be altered by DNL, and this is just what we observed. Indeed, we proved that the effect is basically due to the DNL rather than some intrinsic nonlinearity in the SiPM response; however, such a matter goes beyond the scope of this paper. What is important here is that we managed to overcome this effect by recalibrating the QDC scale by means of a third-order polynomial.

For the sake of completeness, we reproduce the Poisson distribution

$${\rm Poisson}(\mu,n) = \frac{\mu^n}{n!}e^{-\mu}. \tag{3}$$

The fitting procedure exploiting χ^2 minimization for each bias voltage and for each light level allowed one to obtain the three values σ_e, σ_1, and μ. We regret that in a few cases, we had to discard some data, as we later discovered that due to a random electrical interference noise sometimes present in our laboratory, a few measurements were corrupted. Nonetheless, the available data allow us to support a reasonable understanding of the device operation. We also remark that whenever the pedestal peak showed up due to a very low light level, it was not included in the fit procedure in order not to spoil the centroid calibration and the Poissonian shape.

What one expects for each given bias voltage is that σ_1 should somewhat stay constant across the measurements at different light levels, whereas μ should scale rather linearly with the light level; this is what we indeed found out. In Fig. 4, we show the relative electronic noise contribution $\sigma_e/c(1)$ as a function of the bias voltage under different laser intensity conditions. We normalized the absolute σ_e values to the position of the centroid of the $n = 1$ peak in order to get values that can be compared with each other under different conditions of light and bias voltage. Reasonably enough, the electronic noise increases with the bias voltage. The same normalization was applied to the σ_1 values and is shown in Fig. 5. As expected, $\sigma_1/c(1)$ is rather constant, as it basically depends on intrinsic nonuniformities between cells and not on the bias voltage or light level.

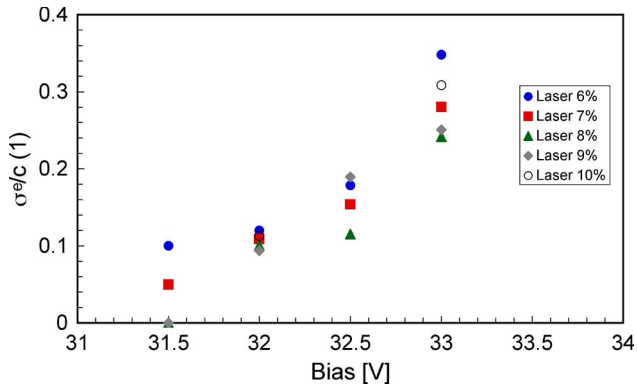

Fig. 4. Relative electronic noise contribution $\sigma_e/c(1)$ as a function of the bias voltage for different laser intensity values. See text for details.

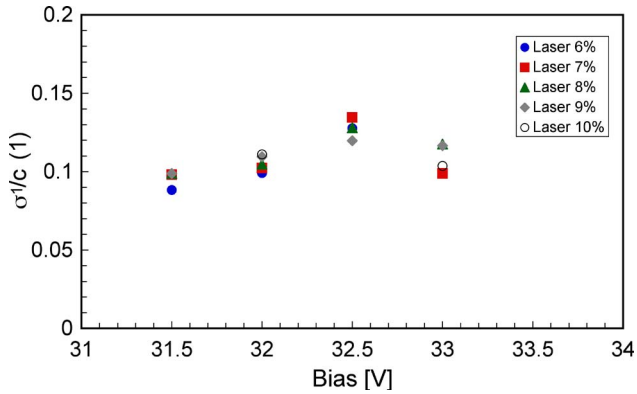

Fig. 5. Relative SiPM noise contribution $\sigma_1/c(1)$ as a function of the bias voltage for different laser intensity values. See text for details.

In Fig. 6, we finally show the overall relative SiPM resolution $\sigma_{\rm tot}(n)/c(n)$ as a function of the number of detected photons for the different bias voltage values.

Having evaluated σ_e and σ_1, we are now capable of computing the photon resolving power of the device under study. If d is the average distance between two consecutive peaks, we can define $R_{3\sigma}$ as the number n of measured photons, where the separation between two consecutive peaks is 3σ. In formulas

$$d = 3\sigma_{\rm tot}(n) \tag{4}$$

and then, from (4) we, can derive

$$n = \frac{1}{\sigma^2_1}\left(\frac{d^2}{9} - \sigma^2_e\right) = R_{3\sigma}. \tag{5}$$

With the same procedure, we can derive $R_{2\sigma}$ that represents the number n of measured photons, where the separation

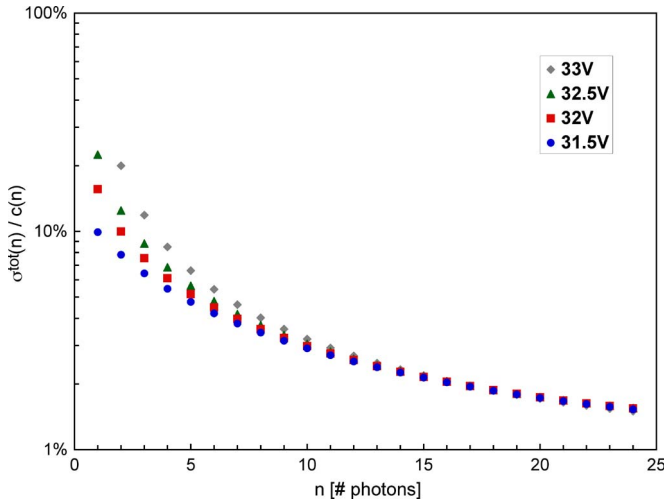

Fig. 6. Relative SiPM resolution $\sigma_{\rm tot}(n)/c(n)$ as a function of the number of detected photons for the different bias voltage values.

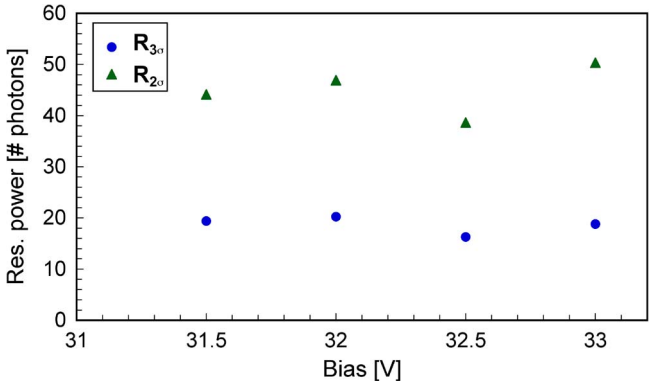

Fig. 7. Photon resolving power $R_{3\sigma}$ of the SiPM under study is the number of measured photons where the separation between two consecutive peaks is a 3σ level; $R_{2\sigma}$ is the number of measured photons where the SiPM resolution becomes 2σ, which means that any hint of separate peaks is lost. See text for further details.

between two consecutive peaks becomes 2σ, which means that any hint of separate peaks is lost.

For our convenience, we define $R_{3\sigma}$ as the photon resolving power of the SiPM under study. Fig. 7 shows that $R_{3\sigma}$ is on the order of 20, whereas $R_{2\sigma}$ is on the order of 45. In practical terms, this means that using this SiPM in our experimental conditions we can clearly separate (3σ level) up to 20 photons, and we still continue to observe separated peaks or structures up to 45 photons (2σ level); beyond that, any resolution on the photon number is lost.

B. Timing Performance

The timing performance of the device is indeed relevant, particularly if we consider that it is easily attained with a very small number of impinging photons. In Fig. 8 (dotted line), we show a sample timing spectrum obtained at a 10% nominal laser intensity and 32-V bias. The time resolution is $\sigma \approx 200$ ps; however, one might wonder if and how it depends on the number of detected photons. Considering that such a question was worth investigating, we proceeded as follows.

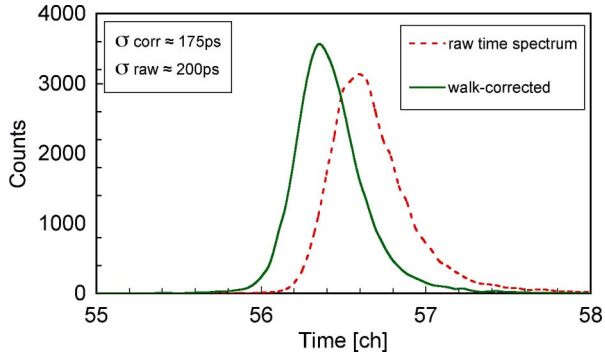

Fig. 8. Timing spectrum obtained at a 10% nominal laser intensity and 32-V bias. The dotted line represents the raw data; the solid line represents the same data after the walk correction as explained in the text.

First off, we built the two charge-time scatter plots shown on the left-hand side of Fig. 9, both taken at a 32-V bias and, respectively, at 5% and 10% nominal laser intensities. As expected, the single-photon peaks stick out as outstanding islands. At a low number of photons, the residual time-walk effect is evident; indeed, the islands are shifted toward longer times due to signals whose amplitude was close to the discriminator threshold (we employed an Ortec CF8000 constant fraction discriminator, which can correct the time walk at the first order but still produces a residual walk). By individually projecting each island onto the time axis, we got several independent time spectra. We fitted these spectra, and the respective widths are shown in Fig. 10. We can see that the time resolution can be as small as 140 ps, particularly if we consider light pulses with more than eight photons detected. A simple fit to the experimental widths shows that the data points are nicely reproduced by a function inversely proportional to the square root of the number of detected photons, as expected. Moreover, Fig. 11 shows the position of the time peak centroid as a function of the number of detected photons. As expected, the time walk shows up clearly. A fit to the data points shows a dependence compatible with a $1/n$ behavior, as expected from the near-threshold signals on a discriminator [25].

Finally, by making use of the fit of Fig. 11, we applied an event-by-event walk correction to the data in order to show how the overall timing can be improved to accommodate a wider range of light intensity. On the right-hand side of Fig. 9 we therefore show the same two charge–time scatter plots after an event-by-event correction for the residual time-walk effect, whereas in Fig. 8 (solid line), we show the overall timing spectrum after applying the same correction.

III. Gain

The SiPM gain is defined as the number of elementary charges (electrons) created in response to the interaction of one photon. Since each cell of the device operates in Geiger mode, the interaction of one photon produces an electron-hole pair, followed by an avalanche multiplication. The avalanche multiplication factor is the gain, and it obviously depends on the bias voltage. As already described in previous papers [21], [26], within the operating range, the gain is expected to grow linearly with the bias voltage.

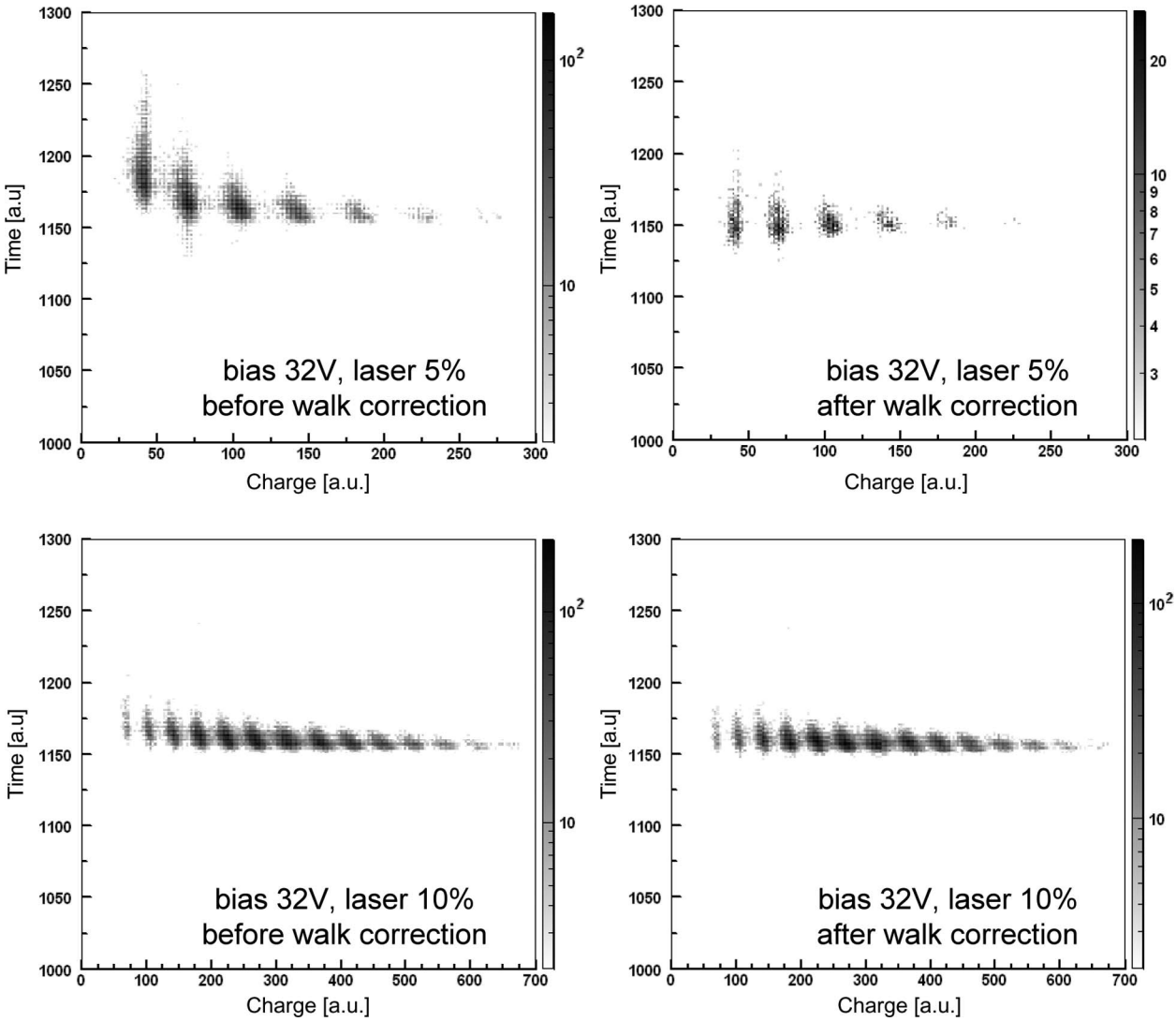

Fig. 9. Charge–time scatter plot at (top) 5% and (bottom) 10% nominal laser intensities and 32-V bias. The left-hand side plots are the raw data before walk correction, and the right-hand side plots are the raw data after walk correction. The photon peaks stick out as outstanding islands. At a (top left plot) low number of photons, the time-walk effect is quite evident.

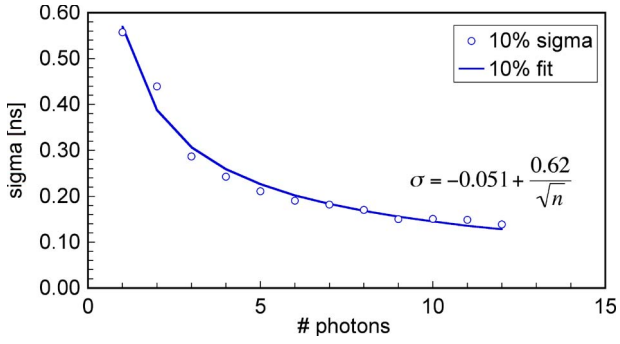

Fig. 10. Time resolution (sigma) as a function of the number of detected photons, with a 10% nominal laser intensity and 32-V bias voltage.

In order to evaluate the gain for each bias value, we computed the average spacing between two consecutive peaks in terms of QDC channels. Then, scaling by the known QDC yield in terms of charge/channel and by the known gain of the employed amplifier, we were able to compute the values shown in Table I

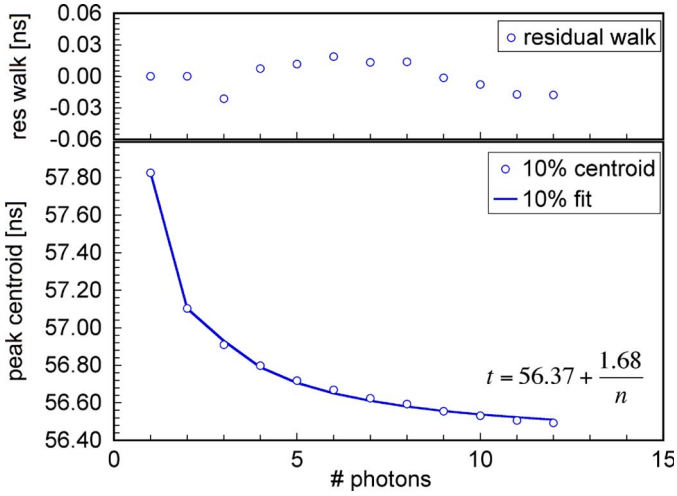

Fig. 11. Time peak centroid as a function of the number of (lower plot) detected photons; the fit result is used to compute the correction needed for the time walk. (Upper plot) Residual walk after the walk correction. The nominal laser intensity was 10%; the bias voltage was 32 V.

TABLE I
SIPM GAIN MEASURED AT THE FOUR REFERENCE BIAS VOLTAGES. SEE TEXT FOR DETAILS ON THE METHOD

Bias voltage	31.5V	32V	32.5V	33V
Average gain	74775	93750	110344	127393

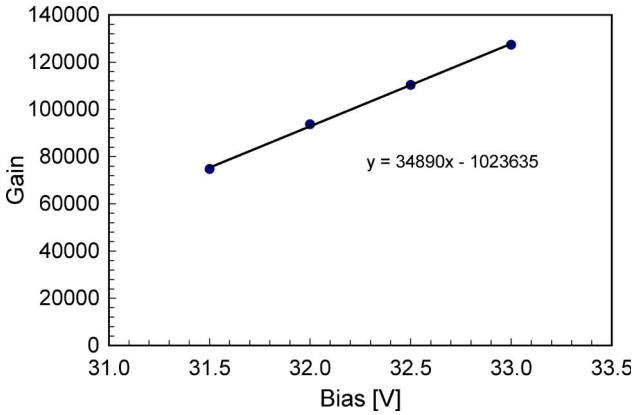

Fig. 12. Gain as a function of the bias voltage. The linear fit allows one to extrapolate the breakdown voltage, i.e., the intercept on the x-axis, as 29.34 V, which is very close to the nominal 29.5 V measured in a totally different fashion by the manufacturer.

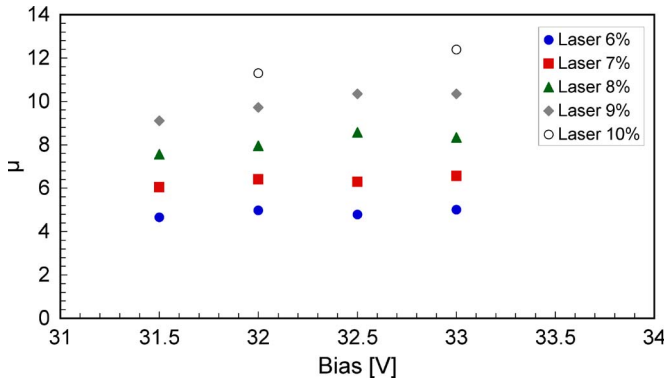

Fig. 13. Average number μ of detected photons as a function of the bias voltage for the four different laser intensity values. The slight increase with the bias voltage is an indication that the PDE increases as well, as expected.

and in Fig. 12. A fit to the data points shows that the behavior is indeed linear. The extrapolation of the intercept on the x-axis gives us an independent estimate of the breakdown value at 29.34 V, very close to the nominal value of 29.5 V measured by the manufacturer in a totally different fashion. This represents, in our opinion, an important cross-check, indicating that our measurement and data-handling procedures are correct.

IV. LINEARITY

In this section, we are going to show that the device response to light is indeed linear. In order to study this behavior, we made use of the μ values obtained by means of our fitting procedure described in Section II-A. Fig. 13 shows the average number μ of detected photons as a function of the bias voltage for different laser intensity values. The slight increase with the bias voltage is an indication that the PDE increases as well, as expected. Fig. 14 shows the average number μ of detected photons as a function of the laser intensity for different bias voltage values. The slope is linear, thus implying the SiPM linear response to light. We remind the reader, however, that this holds only in case the number of fired cells is below $\approx$50% in order to neglect the effect of multiple cell firing [21], [29].

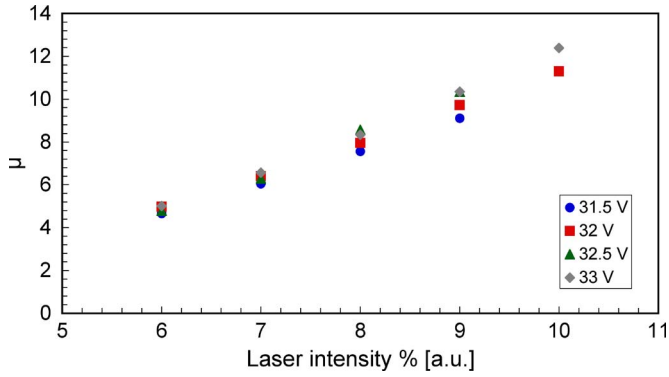

Fig. 14. Average number μ of detected photons as a function of the laser intensity for different bias voltage values. The slope is linear, thus implying the SiPM linear response to light.

Therefore, if we are able to measure the PDE once, as we are going to show in the next section, we will also be able to extrapolate the real number of photons impinging on our sensor from every measurement.

V. PDE

Only a fraction of the photons impinging on the sensor will actually trigger an avalanche and, consequently, a detectable signal [27]. The main reasons for such inefficiencies are geometrical (inactive regions between cells), physical (reflection/absorption by passive layers), and electrical (photon conversion occurring in regions where the electric field is not suitable for triggering the avalanche).

The overall efficiency of the sensor is generally referred to as PDE, and it relates the real number of impinging photons to the measured one based on the following:

$$\mu = \mu_0 \cdot \mathrm{PDE} = \mu_0 \cdot \varepsilon_{\mathrm{geom}} \cdot \varepsilon_{el} \cdot \mathrm{QE} \tag{6}$$

where μ is the just-mentioned average number of detected photons; μ_0 is the true average number of impinging photons; $\varepsilon_{\mathrm{geom}} \approx 0.36$ is the geometrical efficiency of the SiPM and is the only efficiency factor we know with a reasonable precision; $\varepsilon_{\mathrm{el}}$ accounts for the electrical efficiency of the SiPM; and the quantum efficiency (QE) accounts for the physical efficiency.

The measurement we are going to describe allowed us to measure the overall PDE of our SiPM. We employed an optical setup shown in Fig. 15, using a counting electronics scheme. The measurements were performed at room temperature (20 °C). Additional details on the optical setup can be found in [28].

What we basically did was count the photons detected on the SiPM under known light conditions. In order to accomplish this, we selected a given wavelength from the xenon lamp by means of the grating and λ-selection slits. The resulting monochromatic beam was sent into an integrating sphere, which played

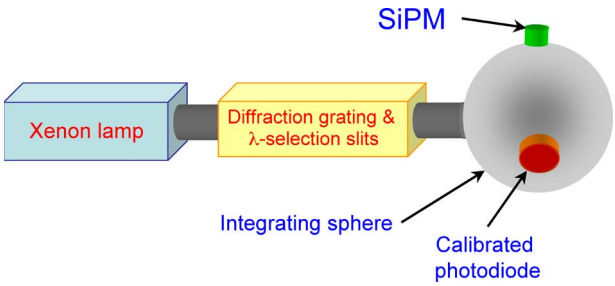

Fig. 15. Scheme of the setup employed for the PDE measurement.

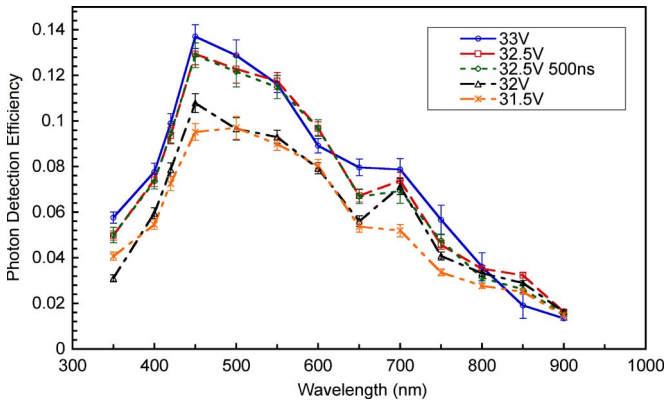

Fig. 16. Overall PDE of the SiPM. See text for the explanation of the 500-ns curve.

the role of randomizer; the internal surface of the sphere was thus uniformly illuminated. Two small apertures on the sphere were used to allocate a reference photodiode (1-cm^2 area) and our SiPM. Using the high-precision calibrated photodiode, we were able to evaluate the absolute number of impinging photons per unit area and then, after proper rescaling, the number of photons impinging onto the SiPM.

By means of neutral filters, we were able to tune the light intensity into the sphere such that we had a well-measurable current on the photodiode and, at the same time, a counting rate on the SiPM of the same order as of its dark noise. The logic signal coming out of the discriminator was given a width of 50 ns, and afterward, the counting rate was corrected for the consequent dead time.

All the errors were duly taken into account and propagated, although the dominant contribution comes from the indetermination of the QE of the reference photodiode.

This measurement was repeated at several different wavelengths and SiPM bias voltages. The resulting PDE values are shown in Fig. 16. In order to verify the reliability of the dead-time correction, we also performed measurements with different durations of the logic signal to the counter. After the correction, the obtained values were not distinguishable from each other, as shown in Fig. 16 where we also show a sample set of PDE values measured at a 32.5-V bias with a 500-ns signal duration. We also checked that the measured PDE values were stable with respect to changes in the primary light intensity. To this purpose, we performed several measurements at fixed wavelength and bias voltage by changing the light level by one order of magnitude. The results, which are not shown, were the same.

VI. Discussion

The results of the charge measurements state that our SiPM has outstanding features, as testified by the 2σ and 3σ resolving power that allows one to distinguish up to $\approx$45 photons at room temperature. Considering that the total number of cells is 100, this is certainly a remarkable result. In addition, we want to mention here that the resolution of our SiPM allowed us to appreciate and corrrect the DNL of the QDC.

As was the case with the noise (see part 1), the charge response is also reproducible and obeys simple mathematical laws; Poisson statistics and Gaussian folding are enough to reproduce our data at all bias voltages and light levels. This also allowed us to evaluate the gain of the sensor, and it being on the order of 10^5, the SiPM is better used with an amplifier. However, we do not exclude producing a new version with increased cell capacitance in order to achieve a higher gain and eliminate the need of the amplifier [29] at the possible cost of the deterioration of the timing.

The linearity was checked against the laser nominal intensity, and it appears quite good (Fig. 14). Certainly, one has to take into account that once the number of fired cells goes beyond $\approx$50% of the total, the multiple-hit effect is no longer negligible, and the response tends to saturate [21], [29].

The timing features are relevant as well, being the time resolution on the order of 100 ps, which is similar to the device described in [12]. Moreover, a combined measurement of time and amplitude allows for an additional time-walk correction that further improves the timing performance, as we have shown. We think it is worth mentioning here that by using our SiPM, we were able to appreciate a systematic time shift of our laser (tens of picoseconds) as a function of its intensity, as expected due to the operating principle of a gain-switching diode laser.

The PDE was reliably measured in a single-photon-counting mode [30], and it confirmed that the process of optimizing the device in the blue region by means of a special front layer was indeed successful. We stress here that the PDE values shown in Fig. 16, with a maximum of around 14%, also include the dominant geometrical efficiency ($\approx$36%), which means a single-cell efficiency just below 40% at 450 nm. Other authors recently reported quite higher PDE values, although warning that such values include crosstalk and afterpulsing [8]. Moreover, the PDE measured in [7] on devices of the same family as in [8] shows rather lower values. With our method, we showed that the single-photon PDE measurement is mandatory if one wants to exclude the misleading contribution of correlated noise to the PDE [31], [32]. Collazuol *et al.* [12] employed a similar method and found the PDE values in reasonable agreement with ours.

However, an overall PDE improvement is foreseen for our next production batches.

VII. Conclusion

We have characterized a novel 100-channel SiPM, coming from an improvement of our previous SPAD technology. The result is a working device with outstanding features in terms of single-photon resolution, timing, PDE, and noise. The

dedicated data-analysis procedure we developed and established allows for the immediate extraction of the relevant parameters for the forthcoming generations of SiPM sensors.

The tests we performed and the features we measured as a function of the bias voltage and of the incident photon flux qualify this device as a very promising one, likely already suitable for physical measurement applications in the field.

ACKNOWLEDGMENT

The authors would like to thank G. Passaro, S. Marino, P. Litrico, and C. Calì of the electronics department at LNS, INFN, whose help in building and assembling the PC boards we employed was invaluable.

REFERENCES

[1] M. Ghioni *et al.*, "Compact active quenching circuit for fast photon counting with avalanche photodiodes," *Rev. Sci. Instrum.*, vol. 67, no. 10, pp. 3440–3448, Oct. 1996.

[2] V. D. Kovaltchouk *et al.*, "Comparison of a silicon photomultiplier to a traditional vacuum photomultiplier," *Nucl. Instrum. Methods Phys. Res. A, Accel. Spectrom. Detect. Assoc. Equip.*, vol. 538, no. 1–3, pp. 408–415, Feb. 2005.

[3] F. Zappa *et al.*, "Principles and features of single-photon avalanche diode arrays," *Sens. Actuators A, Phys.*, vol. 140, no. 1, pp. 103–112, Oct. 2007.

[4] P. Buzhan *et al.*, "Silicon photomultiplier and its possible applications," *Nucl. Instrum. Methods Phys. Res. A, Accel. Spectrom. Detect. Assoc. Equip.*, vol. 504, no. 1, pp. 48–52, May 2003.

[5] V. Golovin and V. Saveliev, "Novel type of avalanche photodetector with Geiger mode operation," *Nucl. Instrum. Methods Phys. Res. A, Accel. Spectrom. Detect. Assoc. Equip.*, vol. 518, no. 1, pp. 560–564, Feb. 2004.

[6] I. Britvitch *et al.*, "Development of scintillation detectors based on avalanche microchannel photodiodes," *Nucl. Instrum. Methods Phys. Res. A, Accel. Spectrom. Detect. Assoc. Equip.*, vol. 571, no. 1/2, pp. 317–320, Feb. 2007.

[7] I. Britvitch *et al.*, "Investigation of a photon counting avalanche photodiode from Hamamatsu photonics," *Nucl. Instrum. Methods Phys. Res. A, Accel. Spectrom. Detect. Assoc. Equip.*, vol. 567, no. 1, pp. 276–280, Nov. 2006.

[8] S. Gomi *et al.*, "Development and study of the multi pixel photon counter," *Nucl. Instrum. Methods Phys. Res. A, Accel. Spectrom. Detect. Assoc. Equip.*, vol. 581, no. 1/2, pp. 427–432, Oct. 2007.

[9] D. Renker, "New trends on photodetectors," *Nucl. Instrum. Methods Phys. Res. A, Accel. Spectrom. Detect. Assoc. Equip.*, vol. 571, no. 1/2, pp. 1–6, Feb. 2007.

[10] A. Heering *et al.*, "Performance of silicon photomultiplers with the CMS HCAL front-end electronics," *Nucl. Instrum. Methods Phys. Res. A, Accel. Spectrom. Detect. Assoc. Equip.*, vol. 576, no. 2/3, pp. 341–349, Jun. 2007.

[11] H. Gast *et al.*, "A high resolution scintillating fiber tracker with SiPM readout," *Nucl. Instrum. Methods Phys. Res. A, Accel. Spectrom. Detect. Assoc. Equip.*, vol. 581, no. 1/2, pp. 423–426, Oct. 2007.

[12] G. Collazuol *et al.*, "Single photon timing resolution and detection efficiency of the IRST silicon photo-multipliers," *Nucl. Instrum. Methods Phys. Res. A, Accel. Spectrom. Detect. Assoc. Equip.*, vol. 581, no. 1/2, pp. 461–464, Oct. 2007.

[13] D. J. Herbert *et al.*, "First results of scintillator readout with silicon photomultiplier," *IEEE Trans. Nucl. Sci.*, vol. 53, no. 1, pp. 389–394, Feb. 2006.

[14] P. Buzhan *et al.*, "Large area silicon photomultipliers: Performance and applications," *Nucl. Instrum. Methods Phys. Res. A, Accel. Spectrom. Detect. Assoc. Equip.*, vol. 567, no. 1, pp. 78–82, Nov. 2006.

[15] *SensL SiPMPlus device for the GlueX project at Jefferson Lab*. [Online]. Available: http://www.sensl.com/Products/

[16] D. M. Taylor, J. C. Jackson, A. P. Morrison, A. Mathewson, and J. G. Rarity, "Characterization of novel active area silicon avalanche photodiodes operating in the Geiger mode," *J. Mod. Opt.*, vol. 51, no. 9/10, pp. 1323–1332, Jun. 2004.

[17] M. Mazzillo *et al.*, "Single photon avalanche photodiodes arrays," *Sens. Actuators A, Phys.*, vol. 138, no. 2, pp. 306–312, Aug. 2007.

[18] P. Finocchiaro *et al.*, "A new generation of low-voltage single-photon micro-sensors with timing capability," *Nucl. Instrum. Methods Phys. Res. A, Accel. Spectrom. Detect. Assoc. Equip.*, vol. 567, no. 1, pp. 83–88, Nov. 2006.

[19] E. Sciacca *et al.*, "Arrays of Geiger mode avalanche photodiodes," *IEEE Photon. Technol. Lett.*, vol. 18, no. 15, pp. 1633–1635, Aug. 2006.

[20] M. Mazzillo *et al.*, "Single photon avalanche photodiodes with integrated quenching resistor," *Nucl. Instrum. Methods Phys. Res. A, Accel. Spectrom. Detect. Assoc. Equip.*, vol. 541, no. 2, pp. 367–373, Jun. 2008.

[21] A. C. Giudice *et al.*, "A process and deep level evaluation tool: Afterpulsing in avalanche junctions," in *Proc. 33rd Conf. Eur. Solid-State Device Res.*, 2003, vol. 1, pp. 347–350.

[22] J. C. Jackson *et al.*, "Toward integrated single-photon-counting microarrays," *Opt. Eng.*, vol. 42, no. 1, pp. 112–118, Jan. 2003.

[23] B. Dolgoshein *et al.*, "Status report on silicon photomultiplier development and its applications," *Nucl. Instrum. Methods Phys. Res. A, Accel. Spectrom. Detect. Assoc. Equip.*, vol. 563, no. 2, pp. 368–376, Jul. 2006.

[24] C. Piemonte *et al.*, "Characterization of the first prototypes of silicon photomultiplier fabricated at ITC-irst," *IEEE Trans. Nucl. Sci.*, vol. 54, no. 1, pp. 236–244, Feb. 2007.

[25] C. Agodi *et al.*, "The HADES time-of-flight wall," *Nucl. Instrum. Methods Phys. Res. A, Accel. Spectrom. Detect. Assoc. Equip.*, vol. 492, no. 1/2, pp. 14–25, Oct. 2002.

[26] P. Finocchiaro *et al.*, "Test of scintillator readout with single photon avalanche photodiodes," *IEEE Trans. Nucl. Sci.*, vol. 52, no. 6, pp. 3040–3046, Dec. 2005.

[27] C. Piemonte, "A new silicon photomultiplier structure for blue light detection," *Nucl. Instrum. Methods Phys. Res. A, Accel. Spectrom. Detect. Assoc. Equip.*, vol. 568, no. 1, pp. 224–232, Nov. 2006.

[28] M. Belluso *et al.*, "Electro-optical characteristics of the Single Photon Avalanche Diode (SPAD)," in *Scientific Detectors for Astronomy 2005, Explorers of the Photon Odyssey*, ser. Astrophysics and Space Science Library, J. E. Beletic, J. W. Beletic, and P. Amico, Eds. New York: Springer-Verlag, 2006, pp. 461–467.

[29] P. Finocchiaro *et al.*, "SPAD-arrays and micro-optics: Towards a real single photon spectrometer," *J. Mod. Opt.*, vol. 54, no. 2/3, pp. 199–212, Jan. 2007.

[30] P. Finocchiaro *et al.*, "Single-photon-counting method for measuring the photon detection efficiency of a silicon photomultiplier," *Opt. Express*. submitted for publication.

[31] P. Finocchiaro *et al.*, *talk given at SORMA West 2008, Berkeley, CA, USA*. paper in preparation.

[32] G. Bonanno *et al.*, *talk given at NDIP 2008, Aix Les Bains, France*. paper in preparation.

Paolo Finocchiaro was born in Catania, Italy, in 1958. He received the B.Sc. degree in nuclear physics from the University of Catania, Catania, in 1982.

For several years, he was a Consultant and Teacher of computer science. He has been with INFN, Catania, since 1984, where he was a Researcher who, in this framework, was responsible for several experiments related to technology and nuclear physics and where, since 1995, he has been with the HADES collaboration, whose collaboration board he currently chairs, and since 1999, he has been Technology Director at the Laboratori Nazionali del Sud. He is the author of about 120 articles on physics and technology journals, along with countless contributions to international conferences. His research interest is currently focused on the development of high-performance SiPM detectors for nuclear physics and industrial applications.

Alfio Pappalardo was born in Catania, Italy, in 1969. He received the M.S. degree in physics from the University of Catania, Catania, in 2002.

He received a fellowship from the University of Catania, where he was a Consultant in sensors for particle beam diagnostics and scintillator detectors. He is currently with STMicroelectronics, Catania, and also with the Laboratori Nazionali del Sud, INFN, Catania. He is the author of many articles and conference contributions focused on systems and photodetectors for very low light intensity detection.

Luigi Cosentino was born in Catania, Italy, in 1970. He received the M.S. degree in physics from the University of Catania, Catania, in 1995.

He is a High School Teacher of electronics. He is currently with the Laboratori Nazionali del Sud, INFN, Catania, under research contracts, where he is dealing with the diagnostics of the radioactive ion beam facility. He is the author of many physics and technology papers and is currently involved in the development of high-sensitivity detection systems for photons and charged particles.

Massimiliano Belluso was born in Catania, Italy, in 1967. He received the Diploma degree in electronics from the Archimede Institute of Catania, Catania, in 1985.

He was with STMicroelectronics for three years, was a High School Teacher of electronics for eight years, and is currently a Senior Electronics Designer with the Osservatorio Astronomico di Catania, INAF, Catania. He is the author of about 40 technical and scientific papers and the holder of one international and one Italian patent. His major research interests include solid-state detectors for astrophysical application, characterization of imaging detector arrays, and related controller design with ASIC and FPGA.

Sergio Billotta was born in Catania, Italy, in 1976. He received the M.S. degree in physics from the University of Catania, Catania, in 2003.

He is currently with the Osservatorio Astronomico di Catania, INAF, Catania, as a Research Collaborator and with STMicroelectronics, Catania, as a Consultant. He is the author of about 15 scientific papers and is currently involved in interferometer and quantum astronomy programs. His major research interest includes solid-state photodetectors.

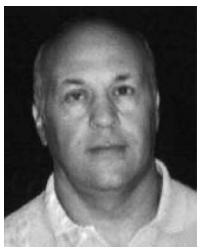

Giovanni Bonanno was born in Catania, Italy, in 1955. He received the B.Sc. degree in physics from the University of Catania, Catania, in 1980.

He has been a Full Astronomer of Astrophysical Technologies with the Ossevatorio Astrofisico di Catania, INAF, Catania, since 2001. He is the author of many papers about detectors and related electronic controllers for astrophysical applications and is the holder of one national patent on a photon-counting system based on a microchannel plate coupled to a CMOS-APS. His research interests are in silicon photodetectors, including charge-coupled devices, single-photon avalanche diodes, silicon photon multipliers, and complementary metal–oxide–semiconductors for ground and space astrophysical applications.

Beatrice Carbone was born in Salerno, Italy, in 1979. She received the M.Sc. degree in physics from the University of Salerno, Salerno, in 2005.

She did her thesis at STMicroelectronics, Catania, Italy, on the development of a special charged-particle silicon detector, which was later tested at the Laboratori Nazionali del Sud, INFN, Catania. She is currently with the R&D DSG, STMicroelectronics. She is the author of several papers and conference contributions and is currently involved in the development of SiPM detectors suitable for positron emission tomography.

Giovanni Condorelli was born in Catania, Italy, in 1972. He received the M.Sc. degree in electronics engineering from the University of Catania, Catania, in 2004, with a thesis regarding the reliability of high-performance CMOS gate insulators.

From 2004 to 2005, he has continued this activity at the Institute for Microelectronics and Microsystems, National Research Council, Catania. He is currently with R&D DSG, STMicroelectronics, Catania, in the field of the development and electrical and structural characterization of photodetectors with electrooptical performances able to fit the requirements needed for industrial and scientific applications.

Salvatore Di Mauro, photograph and biography not available at the time of publication.

Giorgio Fallica received the degree in physics from the University of Catania, Catania, Italy, in 1978.

Since 1981, he has been with STMicroelectronics, where he is currently the Manager of the Dedicated ICs and Advanced Sensors Development Group and where he is also with the R&D DSG. He has 25 years experience in ICs and power electronics development. Since 1988, he managed the development of silicon nuclear particle detectors. He is the author of eight international patents.

Massimo Mazzillo was born in Bari, Italy, in 1976. He received the M.S. degree in semiconductor physics and optoelectronics from the University of Bari, Bari, in 2002.

He is with the R&D DSG, STMicroelectronics, Catania, Italy, where he currently works in the Industrial and Multisegment Research and Development Department. He is the author of several scientific papers about single-photon avalanche photodiodes and is currently involved in the development of silicon single-photon detectors for biomedical and astrophysical applications, as well as silicon carbide photodiodes for ultraviolet light detection.

Alessandro Piazza was born in Catania, Italy, in 1977. He received the M.S. degree in electronic engineering from the University of Catania, Catania, in 2004.

He did his thesis at STMicroelectronics, Catania, working on the design of new structures. He is currently with the R&D DSG, STMicroelectronics, collaborating for the development of a silicon photomultiplier suitable for positron emission tomography.

Delfo Sanfilippo was born in Catania, Italy, in 1969. He received the M.S. degree in physics from the University of Catania, Catania, in 1993.

He was with the Ossevatorio Astrofisico di Catania, INAF, Catania, and with the Radio Astronomy Institute, Noto, Italy, as a Research Collaborator in the field of sensors for astrophysics. Since 1996, he has been with the STMicroelectronics, where he is currently with the R&D DSG. He has a long experience in ICs and power electronics development, and started his activity on photon sensors in 2000. He is the author of several international publications, mainly on smart power devices, silicon light-emitting devices, and single-photon sensors. He holds four international patents.

Giuseppina Valvo was born in Palermo, Italy, in 1971. She received the M.S. degree in physics from the University of Catania, Catania, Italy, in 1996.

Since 1997, she has been with R&D DSG, STMicroelectronics, Catania, as a Sensors Designer, where she has designed and developed several technologies dedicated to detectors. She is currently involved in the development of SiPM photodetectors and is the holder of three international patents.